

## Ge epitaxial films on GaAs (100), (110), and (111) substrates for applications of CMOS heterostructural integrations

Shih-Hsuan Tang, Chien-I Kuo, Hai-Dang Trinh, Edward Yi Chang, Hong-Quan Nguyen, Chi-Lang Nguyen, and Guang-Li Luo

Citation: *Journal of Vacuum Science & Technology B* **31**, 021203 (2013); doi: 10.1116/1.4789427

View online: <http://dx.doi.org/10.1116/1.4789427>

View Table of Contents: <http://scitation.aip.org/content/avs/journal/jvstb/31/2?ver=pdfcov>

Published by the AVS: Science & Technology of Materials, Interfaces, and Processing

---

### Articles you may be interested in

[Structural, morphological, and band alignment properties of GaAs/Ge/GaAs heterostructures on \(100\), \(110\), and \(111\) GaAs substrates](#)

*J. Vac. Sci. Technol. B* **31**, 011206 (2013); 10.1116/1.4770070

[Ultrathin low temperature SiGe buffer for the growth of high quality Ge epilayer on Si\(100\) by ultrahigh vacuum chemical vapor deposition](#)

*Appl. Phys. Lett.* **90**, 092108 (2007); 10.1063/1.2709993

[Influence of regrowth conditions on the hole mobility in strained Ge heterostructures produced by hybrid epitaxy](#)

*J. Appl. Phys.* **96**, 6470 (2004); 10.1063/1.1811784

[Effects of hydrogen annealing on heteroepitaxial-Ge layers on Si: Surface roughness and electrical quality](#)

*Appl. Phys. Lett.* **85**, 2815 (2004); 10.1063/1.1802381

[Si \(100\)- SiO<sub>2</sub> interface properties following rapid thermal processing](#)

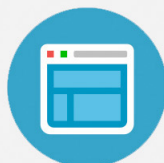
*J. Appl. Phys.* **89**, 3811 (2001); 10.1063/1.1343897

---

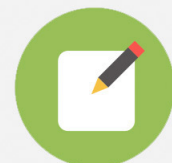


## Re-register for Table of Content Alerts

Create a profile.



Sign up today!



# Ge epitaxial films on GaAs (100), (110), and (111) substrates for applications of CMOS heterostructural integrations

Shih-Hsuan Tang, Chien-I Kuo, Hai-Dang Trinh, Edward Yi Chang,<sup>a)</sup> Hong-Quan Nguyen, and Chi-Lang Nguyen

Department of Materials Science and Engineering, National Chiao Tung University, 1001 Ta-Hsueh Rd., Hsin-chu 300, Taiwan

Guang-Li Luo

National Nano Device Laboratories, Hsin-chu 300, Taiwan

(Received 12 September 2012; accepted 10 January 2013; published 30 January 2013)

Epitaxial Ge films were grown on GaAs (100), (110), and (111) substrates by using ultra-high vacuum chemical vapor deposition and studied with various methods. The incubation times and growth rates were quite different for these three GaAs substrates because the surface arsenic coverage on GaAs and hydrogen desorption energy on Ge are different for each orientation. High-resolution x-ray diffraction measurements, direct band-gap emission of photoluminescence measurements, and cross-sectional transmission electron microscopy showed that the Ge films had high crystal quality, low defect density, and sharp Ge/GaAs interfaces. In this study, atomic force microscopy analysis found that the Ge films grow on GaAs (100) and (111) via the Frank van der Merwe mode, while the Ge film grows on GaAs (110) via the Volmer-Weber mode at the initial growth stage, which can be explained by the thermodynamic theory of capillarity. Interestingly, when the thickness of the Ge film on the GaAs (110) substrate increases to  $\sim 220$  nm, the 3D Ge islands merge and form a smooth surface (rms roughness of 0.3 nm), which is useful for devices. The authors also fabricated Ge metal-oxide-semiconductor capacitors (MOSCAPs) on GaAs (100) and (110) substrates. Both Ge/GaAs (100) and Ge/GaAs (110) MOSCAPs exhibit good capacitance–voltage responses with strong inversion behaviors, which means the grown material has reached device quality. The Ge/GaAs (110) structure especially offers optimal integration of Ge pMOSFETs on GaAs substrates because Ge (110) has a high hole mobility compared with Ge (100) and (111). © 2013 American Vacuum Society. [<http://dx.doi.org/10.1116/1.4789427>]

## I. INTRODUCTION

Device scaling has been a major effort to enhance device performance for semiconductors. Metal–oxide–semiconductor field-effect transistors (MOSFETs) based on III–V materials, such as GaAs and InAs, have recently attracted a lot of attention as n-channel materials because of their high electron mobility compared with strained Si.<sup>1,2</sup> However, III–V materials still suffer from low hole mobility; therefore, it is very important to find a material with high hole mobility for future complementary metal-oxide-semiconductor (CMOS) structures.<sup>3,4</sup> According to the recent the international technology roadmap for semiconductors (ITRS) roadmap,<sup>5</sup> Ge is a good p-channel material. In recent years, several groups have reported growth of Ge on GaAs.<sup>6,7</sup> The main advantage of a Ge epitaxial film grown on GaAs is that the lattice mismatch between these two materials is practically zero ( $\sim 0.08\%$ ), which ensures a large critical thickness, a low dislocation density, and a strain-free Ge epitaxial film.<sup>8</sup> Another characteristic of a Ge film grown on GaAs is that, unlike the growth of a GaAs film on Ge, the film has no anti-phase boundary.<sup>9</sup> Recently, it has been demonstrated that the carrier mobility of a Ge MOSFET can be accelerated by using Ge as a channel with different orientations. For example, Dissanayake *et al.*<sup>10</sup> showed that the hole mobility of

the Ge (110) orientation along the  $\langle 110 \rangle$  directions provides 2.3 times higher hole mobility compared with the Ge (100) surface. Thus, we need to integrate Ge on differently oriented GaAs surfaces to accelerate carrier mobility for future MOSFET applications.

In this study, we grew Ge epitaxial films on GaAs (100), (110), and (111)A substrates using ultra-high vacuum chemical vapor deposition (UHVCVD). The purpose of this study is to investigate the growth mechanisms and crystalline qualities of Ge epitaxial films grown on differently oriented GaAs substrates. In addition, we fabricated and characterized metal-oxide-semiconductor capacitors (MOSCAPs) based on these substrates to demonstrate working devices for future CMOS applications.

## II. EXPERIMENT

We used epi-ready (100), (110), and (111)A GaAs substrates (AXT Inc.) to grow the Ge epitaxial layers. These epi-ready wafers were loaded into the loading chamber of the UHVCVD system without any precleaning. After the pressure of the loading chamber reached  $\sim 2 \times 10^{-7}$  Torr, we transferred each GaAs substrate into the growth chamber and baked it for 90 s at 600 °C prior to deposition of the Ge layer. The purpose of baking is to remove the native oxides (a mixture of As<sub>2</sub>O<sub>3</sub>, As<sub>2</sub>O<sub>5</sub>, and Ga<sub>2</sub>O<sub>3</sub>) from the GaAs surface without any arsenic overpressure. We controlled the baking time carefully to prevent the decomposition of GaAs

<sup>a)</sup> Author to whom correspondence should be addressed; electronic mail: edc@mail.nctu.edu.tw

due to the higher vapor pressure of arsenic.<sup>8</sup> To grow the Ge film, GeH<sub>4</sub> gas was introduced into the chamber at a flow rate of 10 sccm at a fixed pressure of 20 mTorr. The Ge epitaxial film was then deposited on the GaAs substrate at a growth temperature of 600 °C. We then used high-resolution x-ray diffraction (HRXRD), cross-sectional transmission electron microscopy (TEM), and photoluminescence (PL) to investigate the crystal quality and growth rate of the Ge films. In addition, we examined the surface morphology of each Ge film using atomic force microscopy (AFM).

MOS capacitors were also fabricated on Ge films grown on GaAs (100) and (110) substrates using atomic-layer-deposited Al<sub>2</sub>O<sub>3</sub> as the gate dielectric material. The purpose of fabricating the MOSCAP is to verify that the Ge epitaxial film on GaAs (110) can be applied as a channel material with higher hole mobility in further p-MOSFET applications. Prior to fabricating MOSCAPs, we degreased the Ge/GaAs wafer in acetone and isopropanol, followed by dipping in an HF (0.5%) solution for 1 min and rinsing in deionized water. Then, 10 nm of ALD Al<sub>2</sub>O<sub>3</sub> was deposited at 250 °C as the gate dielectric. We carried out postdeposition annealing (PDA) at 400 °C in nitrogen for 5 min and then deposited an e-beam evaporated Ni/Au (500 Å/1000 Å) gate metal and a Ti/Au (500 Å/1000 Å) ohmic contact. Finally, we performed postmetal annealing at 250 °C in nitrogen for 30 s. We measured the capacitance–voltage (C–V) and conductance–voltage (G–V) characteristics of the MOSCAPs using an HP4284A LCR meter.

### III. RESULTS AND DISCUSSION

#### A. Material study and analysis

In our previous study,<sup>8</sup> we found that the growth of Ge on a GaAs (100) substrate has an incubation time. We determined the incubation times of Ge films grown on GaAs substrates by extrapolating the Ge thicknesses versus growth times, as shown in Fig. 1(a).<sup>8,11</sup> In this study, we further found an incubation time in the growth of a Ge film on GaAs (110) and (111) substrates. The incubation times [squares in Fig. 1(b)] of the Ge growth on the GaAs (100), (110), and (111)A substrates at 600 °C are 14.4, 14.2, and 8.3 min, respectively. The growth rates [dots in Fig. 1(b)] of Ge films after the incubation period were 49, 1.2, and 4.7 nm per min on the GaAs (100), (110), and (111)A substrates, respectively. The times required for the growth of a 150-nm Ge epitaxial film on the GaAs (100), (110), and (111)A substrates at 600 °C were 17.4, 140, and 40 min, respectively. The surface configurations of the (100) and (110) GaAs substrates are 50% Ga atom-terminated and 50% As atom-terminated, and the surface configuration of the (111)A GaAs substrate is 100% Ga atom-terminated. Wang *et al.*<sup>12</sup> report that the Ge-Ga dimer has a lower energy state than the Ge-As dimer, and as a consequence, the Ge atoms would easily bond with Ga atoms instead of As atoms. For this reason, longer incubation times would be needed for As desorption on the GaAs (100) and (110) substrates to form Ga-rich surfaces and, thus, enhance the bonding between Ge and Ga atoms. The variation in growth rate between these samples

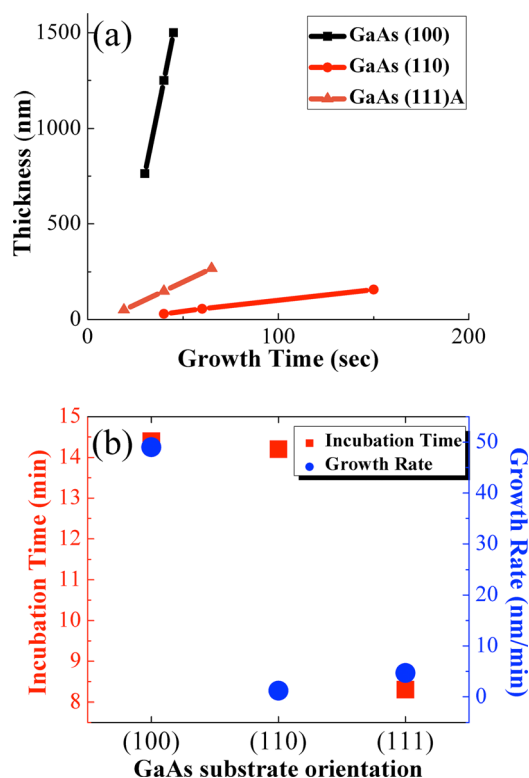


Fig. 1. (Color online) (a) Ge growth thickness vs growth time on GaAs substrates with different orientations. (b) Incubation time (squares) and growth rate (dots) of Ge films grown on GaAs substrates with different orientations.

seems similar to that of the growth of Si and SiGe on Si, as reported by Hartmann *et al.*<sup>13</sup> They suggest that the growth of Si and SiGe on Si (100), (110), and (111) substrates would be affected by the hydrogen (H) desorption in the low-growth-temperature regime. We speculate that the Ge growth on GaAs at 600 °C using GeH<sub>4</sub> is in the H desorption-limited regime, wherein the lower H-atom desorption energy would enhance the Ge growth rate and decrease the activation energy of Ge growth. Therefore, the difference in the Ge growth rate on GaAs substrates is determined by the difference in H-atom desorption energies for Ge (100), (110), and (111) surfaces (after incubation, the GaAs substrate would be fully covered by Ge atoms). These H atoms result from decomposition of the GeH<sub>4</sub> precursor during the growth of the Ge epitaxial film.

We used HRXRD to characterize the quality of the 150-nm-thick Ge epitaxial films deposited at 600 °C on differently oriented GaAs substrates. The results shown in Fig. 2 are for nominal 150-nm-thick Ge films grown on GaAs (100), (110), and (111)A substrates with the GaAs peak set at zero. The HRXRD result and simulated curve in Fig. 2 agree with each other in all three cases, indicating that the Ge epitaxial films grown on GaAs are close to the ideal situation. The appearance of Pendellösung fringes on both sides of the Ge and GaAs peaks indicates a parallel and very sharp heterointerface in this Ge/GaAs heterojunction.<sup>8,12</sup> Calculation using the XRD Pendellösung fringes yields thicknesses of 147.1, 157.2, and 157.6 nm for the Ge films grown on the GaAs (100), (110), and (111)A substrates, respectively.

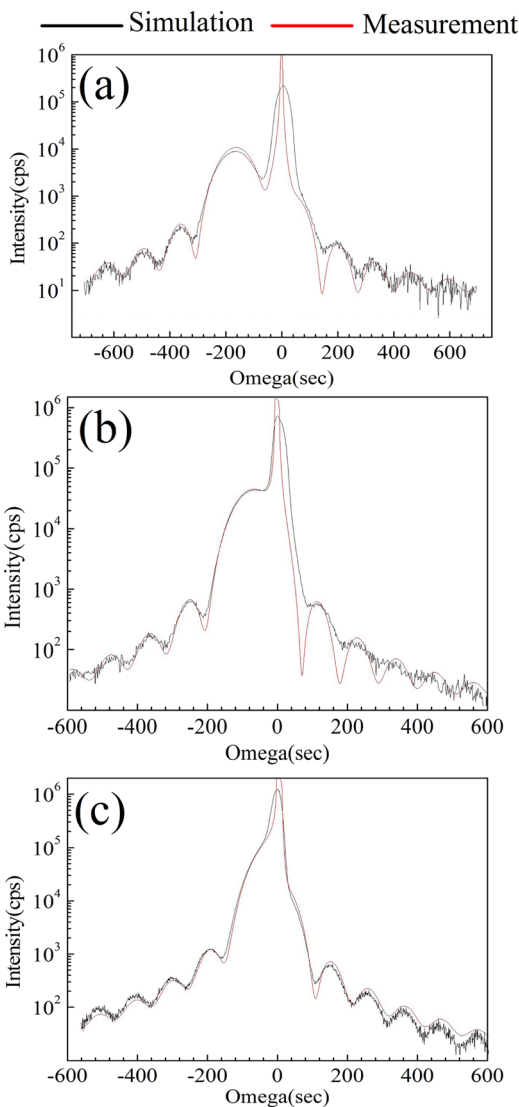


FIG. 2. (Color online) XRD measurement of 150-nm-thick Ge epitaxial films on (a) GaAs (100), (b) GaAs (110), and (c) GaAs (111)A substrates. The black and red lines represent the HRXRD data and simulated curve, respectively. The Pendellösung fringes on both sides imply a sharp and parallel Ge/GaAs interface.

To perform the room-temperature PL measurement, we also grew 1- $\mu\text{m}$  thick Ge films on all three GaAs substrates. From a previous study,<sup>8</sup> it is known that the Ge films are all n-type because of an arsenic autodoping effect during the growth of the Ge epitaxial film on GaAs, and n-type doping of Ge will compensate the 0.136-eV difference in energy between the  $\Gamma$  and L valleys of Ge to cause a direct radiative transition. In addition, the direct radiative transition rate is about 1600 times higher than that of the indirect transition at high-power excitation in the PL measurement.<sup>14</sup> Figure 3 is the PL infrared spectrum of 1- $\mu\text{m}$  thick Ge on the (100), (110), and (111) GaAs substrates with 330-mW PL incident laser power. The PL peak at 0.8 eV reveals that the electrons in the T valley recombine with holes in the valence band,<sup>8</sup> so the direct band-gap emission occurs in all 1- $\mu\text{m}$  Ge films on GaAs substrates. Also, the emission that occurs from 650 to 750 meV is indirect emission, which has much lower inten-

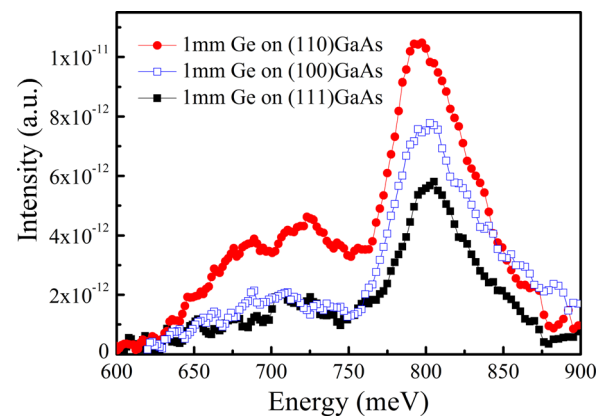


FIG. 3. (Color online) PL infrared spectrum of Ge epitaxial films on (100), (110), and (111) GaAs substrates with 330-mW PL incident laser power.

sity than the direct band emission. The detection of direct emission in the PL measurement indicates that the defect densities of the Ge films on (100), (110), and (111) GaAs substrates are very low. Otherwise, nonradiative recombination due to the large number of defects would decrease the intensity of the PL emission.

We measured the surface morphologies of each 150-nm-thick Ge film using tapping-mode AFM, as shown in Fig. 4. The root mean square (rms) roughness of Ge epitaxial films on the GaAs (100), (110), and (111)A substrates was 0.16, 9.9, and 0.2 nm, respectively, and the mean surface roughness (Ra) was 0.12, 8.5, and 0.16 nm, respectively. Figure 4 shows that, unlike the surface roughness of Ge films grown on (100) and (111)A substrates, the surface morphology of the Ge epitaxial film grown on the (110) GaAs substrate is very rough and 3D-like, even though the lattice constants of Ge and GaAs are almost the same.

We used cross-sectional TEM to characterize further the crystalline qualities of the 150-nm-thick Ge films grown at 600  $^{\circ}\text{C}$  on differently oriented GaAs substrates (Fig. 5). This figure shows no threading dislocations in the Ge epitaxial films grown on these off-oriented GaAs substrates, and the films exhibit excellent Ge/GaAs heterointerfaces. Thus, the surface roughness of the Ge film on the GaAs (110) substrate is not caused by strain relaxation, since no dislocations were observed in the Ge film. Also, the Ge films grown on GaAs (100), (110), and (111)A substrates are defect-free and have good crystalline quality.

To further understand the mechanism and growth mode of Ge films on GaAs substrates with different orientations, we prepared Ge films with the same growth time of 60 min for AFM measurements. Figure 6 shows the results. The thicknesses of the Ge films grown on the (100), (110), and (111)A GaAs were 2234, 55, and 243 nm, respectively, after 60 min of growth. The root mean square roughnesses of Ge epitaxial films on the GaAs (100), (110), and (111)A substrates were 0.3, 0.9, and 0.2 nm, respectively, and the mean surface roughnesses of the films were 0.2, 0.73, and 0.17 nm, respectively. From the AFM analysis in Figs. 6(a) and 6(c), we see that the Ge growth on GaAs (100) and (111)A substrates is a 2D growth, i.e., the Ge surfaces remain flat during



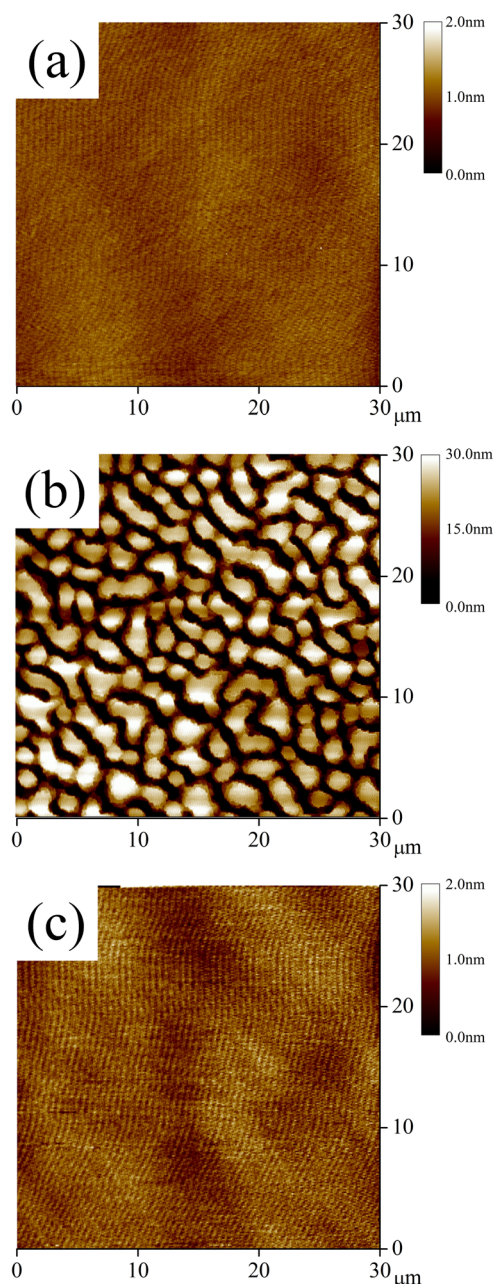


FIG. 4. (Color online) AFM measurement of 150-nm-thick Ge epitaxial films on (a) GaAs (100), (b) GaAs (110), and (c) GaAs (111)A substrates. The scale of each figure is  $30 \mu\text{m} \times 30 \mu\text{m}$ .

the whole growth process. In Fig. 6(b), it is obvious that the growth mode on the GaAs (110) substrate is island growth (3D growth). To compare the effect of growth temperature on the Ge surface morphology on GaAs (110) substrates, we also attempted to grow the Ge film at a low temperature of  $450^\circ\text{C}$ . From the AFM analysis (not shown here), we can see that the growth mode of the Ge film at low temperatures is still island growth, which is independent of temperature.

The growth mode difference of epitaxial Ge for different orientations of GaAs substrates can be explained by the thermodynamic theory of capillarity.<sup>15</sup> The growth mode would depend on the Ge film surface energy ( $\gamma_f$ ), the inter-

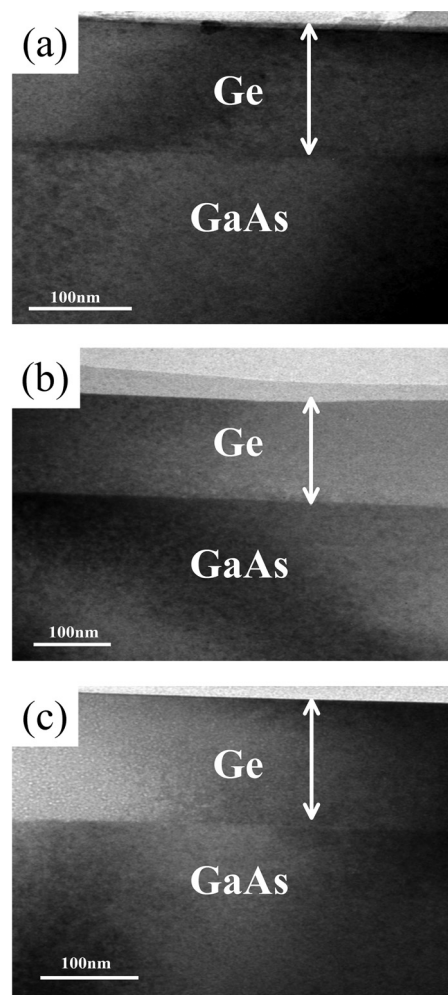


FIG. 5. Cross-sectional TEM image of 150-nm-thick Ge grown on (a) GaAs (100), (b) GaAs (110), and (c) GaAs (111)A substrates. No threading dislocations are detected in any of the Ge films.

facial energy between Ge and GaAs surface ( $\gamma_i$ ), and the GaAs substrate surface energy ( $\gamma_s$ ). Frank van der Merwe growth (2D growth) occurs only when  $\Delta\gamma = \gamma_f + \gamma_i - \gamma_s \leq 0$ . In the opposite extreme, one obtains Vomer-Weber growth (3D growth) when  $\Delta\gamma = \gamma_f + \gamma_i - \gamma_s > 0$ . In the GaAs/Ge heteroepitaxial system, because the lattice constant is almost the same, the interfacial energy (or tension) between the Ge film and the substrate is negligible ( $\gamma_i = 0$ ). Moll *et al.*<sup>16</sup> have calculated the surface energies of different orientations of GaAs surfaces. When the GaAs (100) surface is baked, the phase of the GaAs surface transfers to a Ga-rich ( $4 \times 2$ ) reconstruction, and the energy of the Ga-rich (100) surface is  $1.056 \text{ J/m}^2$ . The energy of (110) GaAs with a cleavage surface is  $0.832 \text{ J/m}^2$ . While the surface of GaAs (111) is Ga-rich, the surface energy is  $1.488 \text{ J/m}^2$ . Stekolnikov *et al.*<sup>17</sup> have reported the Ge surface energy for various orientations and reconstructions. The surface energies of Ge (100)  $7 \times 7$ , Ge (110) and Ge (111)  $2 \times 1$  are 1.02, 1.17, and  $1.05 \text{ J/m}^2$ , respectively. One can determine the growth mode of Ge grown on a GaAs substrate by comparing the surface energy between GaAs and Ge with various orientations. For Ge grown on GaAs (100) and (111)

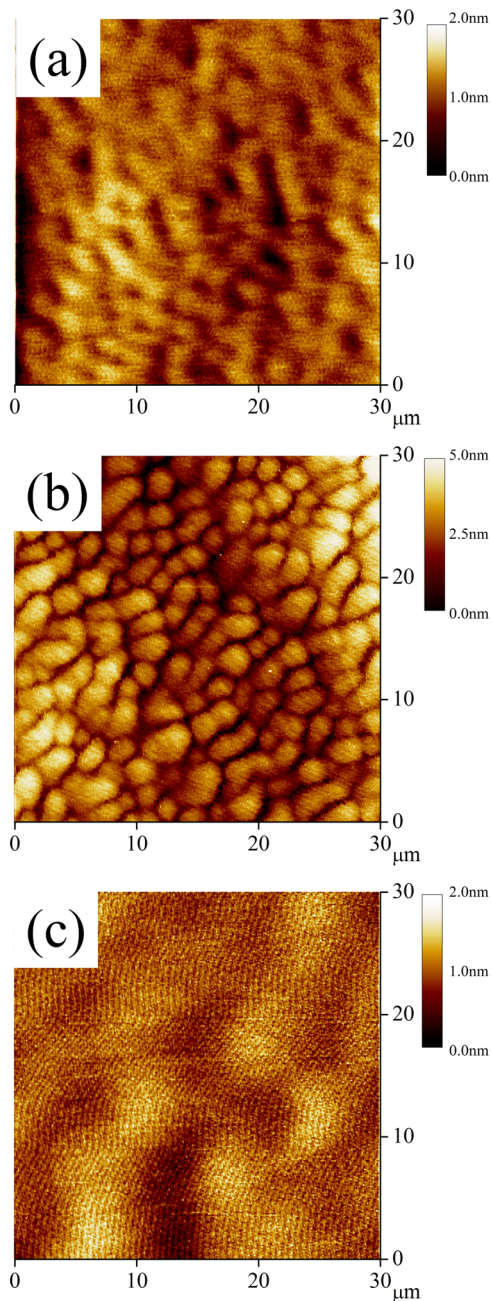


Fig. 6. (Color online) AFM measurement of Ge epitaxial films grown for 60 min on (a) GaAs (100), (b) GaAs (110), and (c) GaAs (111)A substrates. The thicknesses of the Ge film are 2234, 55, and 243 nm, respectively. The scale of each figure is  $30 \mu\text{m} \times 30 \mu\text{m}$ .

substrates, the surface energy of Ge is smaller than that of the GaAs substrate and, from the thermodynamic theory of capillarity, the growth mode must be Frank van der Merwe growth ( $\Delta\gamma = \gamma_f - \gamma_s \leq 0$ ). For the growth of Ge on a GaAs (110) substrate, it is obvious that the surface energy of Ge (110) is larger than that of GaAs (110), which means 3D Ge islands would form to reduce the total surface energy. Moreover, from the capillarity theory, the inequality of the surface energies ( $\Delta\gamma = \gamma_f - \gamma_s > 0$ ) indicates that the growth mode of Ge on the GaAs (110) surface is Volmer-Weber growth (3D growth).

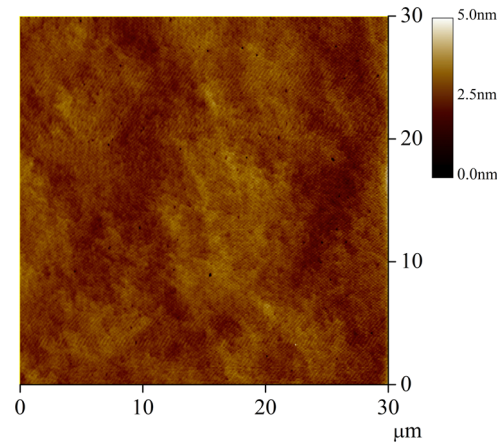


Fig. 7. (Color online) AFM measurement of a 220-nm-thick Ge epitaxial film on a GaAs (110) substrate. The rms roughness and Ra values are 0.37 and 0.26 nm, respectively.

Since the rough Ge (110) film is not suitable for device application, we further studied the growth of Ge on GaAs (110), focusing on improving the Ge surface roughness. As shown in Fig. 6(b), the 55-nm Ge film grown on GaAs (110) is island-like. When the thickness of the Ge film reaches 150 nm [Fig. 4(b)], the surface of the Ge film on GaAs (110) is rougher because of the formation of 3D islands with flat plateau-like surfaces. However, with continuing growth, the 3D islands start to merge. We found that when the thickness of the Ge film on the GaAs (110) substrate was increased to  $\sim 220$  nm, the growth mode switched entirely to 2D growth, as shown by the AFM image in Fig. 7. It is obvious that the islands are all merged, forming a smooth surface with rms roughness and Ra values of 0.37 and 0.26 nm, respectively. This interesting result is very encouraging because it implies the possibility of applying Ge/GaAs (110) p-channel devices, since Ge (110) has a higher hole mobility than Ge (100) and (111) films.

## B. Ge/GaAs MOSCAP

Figure 8 shows the C-V curves of  $\text{Al}_2\text{O}_3/150\text{-nm Ge}/\text{GaAs (100)}$  and  $\text{Al}_2\text{O}_3/220\text{-nm Ge}/\text{GaAs (110)}$  MOSCAPs with smooth Ge surfaces measured at frequencies from 100 Hz to 1 MHz to check the quality of the Ge film and the interface between the Ge film and  $\text{Al}_2\text{O}_3$ . In addition, the measurement could show the feasibility of using the Ge epitaxial film as a channel material on a GaAs (110) substrate to accelerate hole mobility. The C-V responses in the two MOSCAPs show n-type behavior, which indicates n-type doping in the Ge epitaxial layer. This agrees with the previous study and is related to the arsenic auto-doping effect during the growth of the Ge epitaxial film on GaAs.<sup>8</sup> Both samples show smooth C-V curves with good inversion behaviors and a smaller frequency dispersion in the accumulation region. From the G-V measurement, we find the interface trap density,  $D_{it}$ , near the midgap to be about  $1 \times 10^{12} \text{cm}^{-2} \text{eV}^{-1}$ , as estimated by the conductance method. This demonstrates the potential of Ge for MOSCAP applications with higher carrier



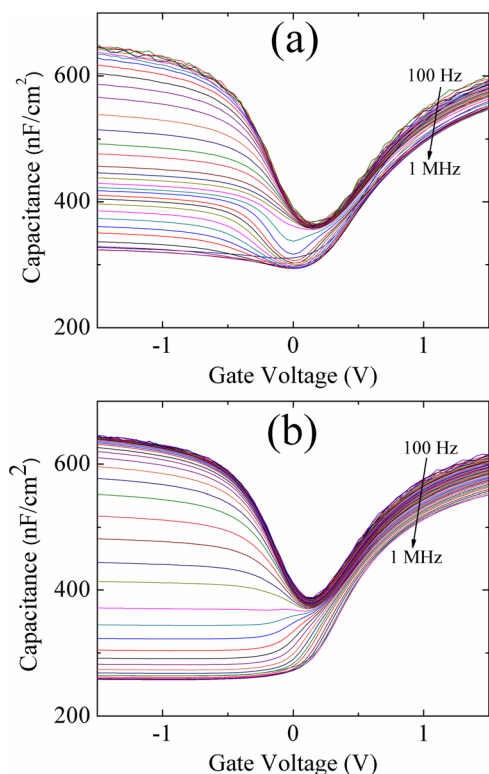


Fig. 8. (Color online) Capacitance–voltage measurement of (a)  $\text{Al}_2\text{O}_3/150\text{-nm Ge/GaAs (100)}$  and (b)  $\text{Al}_2\text{O}_3/220\text{-nm Ge/GaAs (110)}$  MOSCAPs at frequencies from 100 Hz to 1 MHz.

mobility and, thus, future integration into beyond-CMOS logic applications.

#### IV. CONCLUSIONS

We successfully grew high-crystalline-quality Ge epitaxial films on (100), (110), and (111) GaAs substrates using UHVCVD. The differences in incubation time and Ge growth rate on differently oriented GaAs substrates are affected by the surface arsenic coverage on GaAs and the hydrogen desorption energy on Ge, respectively. The XRD, PL, and TEM measurements indicated high-quality defect-free Ge films grown on differently oriented GaAs substrates. The Ge films on the GaAs (100) and (111) substrates were smooth with small rms roughness and Ra values, regardless of the Ge thickness. We found that the growth of the Ge film on GaAs (100) and (111) is in the Frank van der Merwe

mode, while the growth of the Ge film on GaAs (110) is in the Volmer-Weber mode at the initial growth stage, which can be explained by the thermodynamic theory of capillarity. When the thickness of the Ge film on the GaAs (110) substrate increases to  $\sim 220\text{ nm}$ , the 3D Ge islands merge and form a smooth surface (rms roughness of  $0.3\text{ nm}$ ). The  $\text{Al}_2\text{O}_3/150\text{-nm Ge/GaAs (100)}$  and  $\text{Al}_2\text{O}_3/220\text{-nm Ge/GaAs (110)}$  MOSCAPs with smooth Ge surfaces show smooth C-V curves with good inversion behaviors and small frequency dispersions in the accumulation and depletion regions. This study helps integrate Ge p-channel and III-V n-channel MOSFETs on the same GaAs template for beyond-Si-CMOS logic applications.

#### ACKNOWLEDGMENTS

The authors would like to thank Professor C. W. Liu of EE/NTU for PL measurements and Professor Mantu K. Hudait of ECE/Virginia Tech for discussion of this work.

- <sup>1</sup>C. I. Kuo, H. T. Hsu, and E. Y. Chang, *Electrochem. Solid-State Lett.* **11**, H193 (2008).
- <sup>2</sup>H.-C. Chin, X. Gong, L. Wang, H. K. Lee, L. Shi, and Y.-C. Yeo, *IEEE Electron Device Lett.* **32**, 146 (2011).
- <sup>3</sup>E. A. Fitzgerald, *Mater. Sci. Eng. B* **124**, 8 (2005).
- <sup>4</sup>T. Akatsu et al., *Mater. Sci. Semicond. Process.* **9**, 444 (2006).
- <sup>5</sup>J. Hutchby, *ITRS Public Conference: Emerging Research Devices*, Songdo City, Incheon, Korea, 14 December 2011 (Taiwan Semiconductor Industry Association (TSIA), Taiwan), p. 12.
- <sup>6</sup>M. Zhu, H. C. Chin, G. S. Samudra, and Y. C. Yeo, *J. Electrochem. Soc.* **155**, H76 (2008).
- <sup>7</sup>Y. Bai, K. E. Lee, C. W. Cheng, M. L. Lee, and E. A. Fitzgerald, *J. Appl. Phys.* **104**, 084518 (2008).
- <sup>8</sup>S. H. Tang, E. Y. Chang, M. Hudait, J. S. Maa, C. W. Liu, G. L. Luo, H. D. Trinh, and Y. H. Su, *Appl. Phys. Lett.* **98**, 161905 (2011).
- <sup>9</sup>G. L. Luo, Y. C. Hsieh, E. Y. Chang, M. H. Pilkuhn, C. H. Chien, T. H. Yang, C. C. Cheng, and C. Y. Chang, *J. Appl. Phys.* **101**, 084501 (2007).
- <sup>10</sup>S. Dissanayake, Y. Zhao, S. Sugahara, M. Takenaka, and S. Takagi, *J. Appl. Phys.* **109**, 033709 (2011).
- <sup>11</sup>G.-L. Luo et al., *J. Electrochem. Soc.* **157**, H27 (2010).
- <sup>12</sup>X. S. Wang, K. W. Self, and W. H. Weinberg, *J. Vac. Sci. Technol. A* **12**, 1920 (1994).
- <sup>13</sup>J. M. Hartmann, M. Burdin, G. Rolland, and T. Billon, *J. Cryst. Growth* **294**, 288 (2006).
- <sup>14</sup>T. H. Cheng, C. Y. Ko, C. Y. Chen, K. L. Peng, G. L. Luo, C. W. Liu, and H. H. Tseng, *Appl. Phys. Lett.* **96**, 091105 (2010).
- <sup>15</sup>O. Manasreh, *Semiconductor Heterojunction and Nanostructures* (McGraw Hill, Asia, 2005).
- <sup>16</sup>N. Moll, A. Kley, E. Pehlke, and M. Scheffler, *Phys. Rev. B* **54**, 8844 (1996).
- <sup>17</sup>A. A. Stekolnikov, J. Furthmüller, and F. Bechstedt, *Phys. Rev. B* **65**, 115318, (2002).